RESEARCH ARTICLE

NEUROSCIENCE

Inhibition of mTOR Signaling in Parkinson's Disease Prevents L-DOPA–Induced Dyskinesia

Emanuela Santini,[1] Myriam Heiman,[2] Paul Greengard,[2] Emmanuel Valjent,[1,3,4,5] Gilberto Fisone[1,2]*

Parkinson's disease (PD), a disorder caused by degeneration of the dopaminergic input to the basal ganglia, is commonly treated with L-DOPA. Use of this drug, however, is severely limited by motor side effects, or dyskinesia. We show that administration of L-DOPA in a mouse model of Parkinsonism led to dopamine D1 receptor–mediated activation of the mammalian target of rapamycin (mTOR) complex 1 (mTORC1), which is implicated in several forms of synaptic plasticity. This response occurred selectively in the GABAergic medium spiny neurons that project directly from the striatum to the output structures of the basal ganglia. The L-DOPA–mediated activation of mTORC1 persisted in mice that developed dyskinesia. Moreover, the mTORC1 inhibitor rapamycin prevented the development of dyskinesia without affecting the therapeutic efficacy of L-DOPA. Thus, the mTORC1 signaling cascade represents a promising target for the design of anti-Parkinsonian therapies.

INTRODUCTION

The main pathological feature of Parkinson's disease (PD) is the degeneration of midbrain dopaminergic neurons located in the substantia nigra, which project to the dorsal striatum (1). The loss of nigrostriatal input is accompanied by profound modifications in the response of GABAergic medium spiny neurons (MSNs) to drugs that modulate dopaminergic signaling, including L-DOPA, the most effective anti-Parkinsonian medication (2–4). Prominent among these changes is the activation of the two mitogen-activated protein kinases (MAPKs), extracellular signal–regulated kinase (ERK) 1 and 2 (5–8), which are involved in various types of synaptic plasticity (9). Persistent activation of ERK in striatal MSNs leads to the development of dystonic and choreic motor complications, or dyskinesia, which limits the use of L-DOPA as an anti-Parkinsonian therapy (7, 10). The ability to interfere with the striatal signaling machinery controlled by ERK presents a key target for the design of anti-Parkinsonian therapies.

Accumulating evidence indicates that ERK participates in the activation of the mammalian target of rapamycin (mTOR), a key regulator of protein synthesis, which promotes 5′ cap-dependent initiation of messenger RNA (mRNA) translation (11). mTOR regulates translation after the formation of an mTOR complex 1 (mTORC1) containing mTOR and the rapamycin-sensitive adaptor protein of mTOR, Raptor (11). In the hippocampus, mTORC1-dependent signaling has been implicated in the development of the late phase of long-term potentiation, through increased activity of the dendritic translation machinery (12, 13). Moreover, L-DOPA–induced dyskinesia (LID) has been associated with loss of depotentiation at the corticostriatal synapses of MSNs, which results in persistent enhancement of synaptic efficiency (14). These observations led us to hypothesize that some of the adaptive processes responsible for dyskinesia may involve dysregulation of mTORC1 by L-DOPA.

Here, we show that lesion of the nigrostriatal pathway, a well-established model of Parkinsonism, conferred to L-DOPA the ability to activate mTOR signaling in a subset of dopamine D1 receptor (D1R)–positive MSNs that directly innervate the output structures of the basal ganglia. In addition, mTORC1-mediated phosphorylation was associated with the dyskinesia produced by chronic treatment with L-DOPA, and administration of rapamycin, an mTORC1 inhibitor, counteracted the development of this motor complication.

RESULTS

L-DOPA induces phosphorylation of S6 kinase and ribosomal protein S6 in the dopamine-depleted striatum

mTOR has been implicated in the response to a variety of cell signaling molecules, but at present, little is known about the ability of dopaminergic drugs to affect mTOR signaling in the striatum. We examined the effect of L-DOPA on the mTORC1 signaling cascade in mice lesioned unilaterally with 6-hydroxydopamine (6-OHDA), a toxin used to produce a Parkinsonian model in rodents (15, 16). The choice of this model was based on previous evidence showing that repeated administration of L-DOPA to hemi-Parkinsonian mice (which have unilateral lesions of striatal dopaminergic fibers) results in the appearance of asymmetrical abnormal involuntary movements (AIMs), which represent a behavioral correlate for LID (17).

mTORC1 activates the p70 S6 kinase (S6K), which is responsible for the phosphorylation of the ribosomal protein S6 (S6), a component of the 40S ribosomal subunit (18). Administration of L-DOPA (20 mg/kg) in combination with benserazide (12 mg/kg) to 6-OHDA–lesioned mice increased S6K phosphorylation at Thr^{389}, a site directly regulated by mTOR, thereby increasing kinase activity (19) (Fig. 1). This effect was dependent on depletion of striatal dopamine, because L-DOPA did not modify S6K phosphorylation in sham-lesioned mice. Moreover, lesion with 6-OHDA in the absence of L-DOPA did not affect the amount of phospho-Thr^{389}-S6K (Fig. 1A). Total amounts of S6K were unaffected by treatment with 6-OHDA or L-DOPA (Fig. 1A). Similar results were obtained when phosphorylation of S6 was assessed at Ser^{240} and Ser^{244} ($Ser^{240/244}$), sites specifically regulated by S6K, and at Ser^{235} and Ser^{236}

[1]Department of Neuroscience, Karolinska Institutet, Retzius väg 8, 171 77 Stockholm, Sweden. [2]Laboratory of Molecular and Cellular Neuroscience, The Rockefeller University, New York, NY 10021, USA. [3]INSERM, UMR-S839, 75005 Paris, France. [4]Université Pierre et Marie Curie, 75005 Paris, France. [5]Institut du Fer à Moulin, 75005 Paris, France.
*To whom correspondence should be addressed. E-mail: gilberto.fisone@ki.se

Fig. 1. L-DOPA induces D1R-dependent phosphorylation of S6K and S6 in the striata of 6-OHDA–lesioned mice. (**A** and **B**) Quantification of phospho (P)-Thr[389]-S6K, P-Ser[240/244]-S6, and P-Ser[235/236]-S6 in the striata of sham-lesioned mice (Sham) or 6-OHDA–lesioned mice treated with saline, L-DOPA, L-DOPA plus SCH23390 (SCH), or L-DOPA plus raclopride (Rac). Representative Western blots of phosphorylated and total proteins are shown (left). Error bars represent SEM [(A) n = 12 to 24 mice per treatment, (B) n = 7 to 14 mice per treatment] of data calculated as percent of Sham treated with saline. Statistical significance was determined by two-way (A) and one-way ANOVA (B) followed by the Bonferroni–Dunn test. ***P < 0.001 versus Sham treated with saline. (**C** and **D**) Immunofluorescent detection (C) and quantification (D) of cells positive for P-Ser[240/244]-S6 and P-Ser[235/236]-S6 in the striata of Sham and 6-OHDA–lesioned mice treated with L-DOPA alone or in combination with SCH23390 (SCH) or raclopride (Rac). Scale bar, 40 μm. Error bars represent SEM (n = 3 mice per treatment). Statistical significance was determined by one-way ANOVA followed by the Bonferroni–Dunn test. ***P < 0.001 versus Sham treated with L-DOPA.
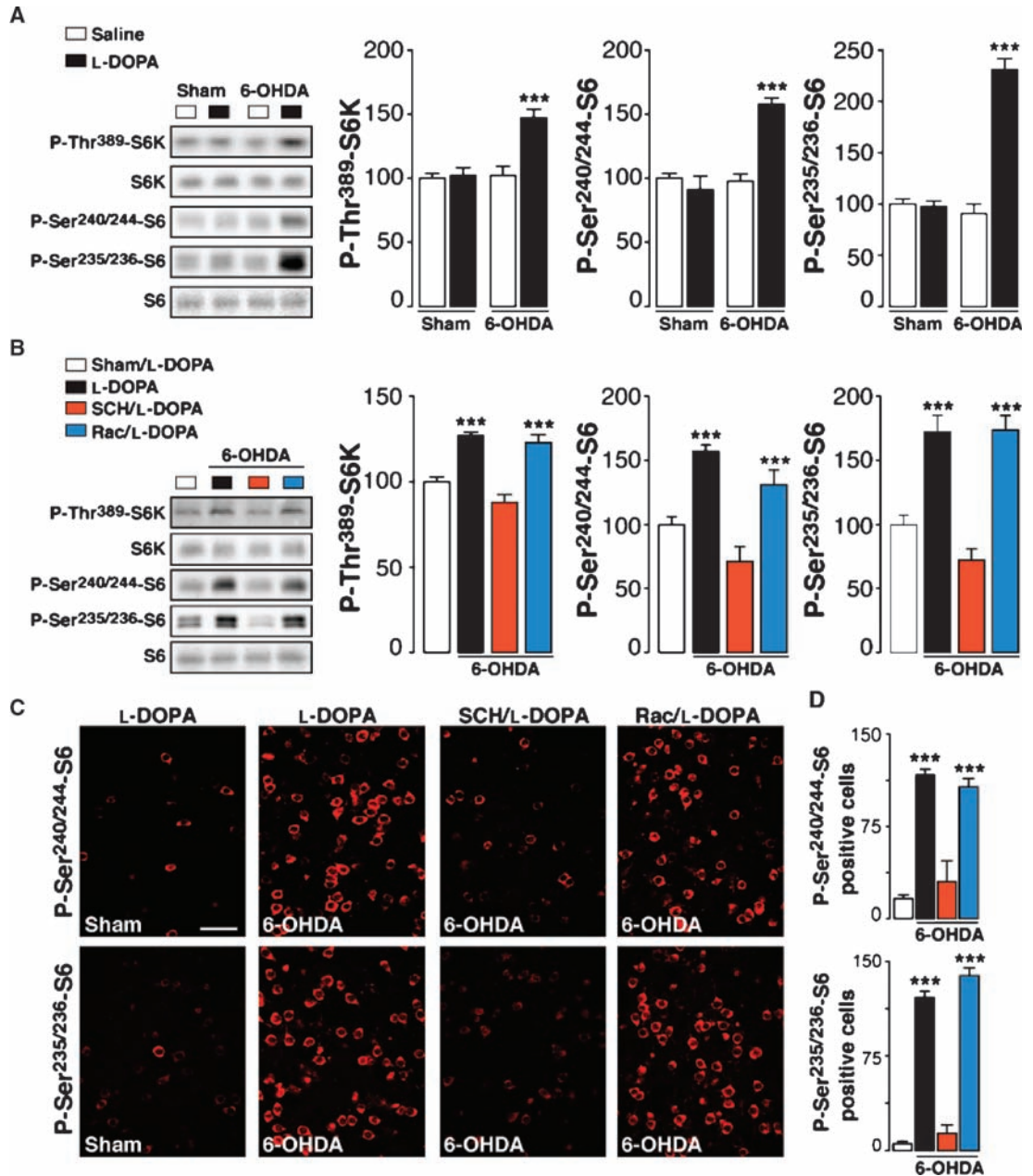
(Ser[235/236]), sites regulated by S6K and ERK (*20*) (Fig. 1A). Phosphorylation at both sets of sites is thought to activate S6 (*20*).

L-DOPA phosphorylates S6 in D1R-containing MSNs of the direct pathway

The effects of L-DOPA are secondary to its conversion to dopamine. In the striatum, increased dopamine concentrations activate D1Rs and dopamine D2 receptors (D2Rs), which are abundant in MSNs (*21*). We examined the possible involvement of these receptors in the phosphorylation of S6K and S6 induced by L-DOPA. Administration of the D1R antagonist, SCH23390 (0.125 mg/kg ip), abolished the L-DOPA–induced increases in phosphorylation of both proteins. In contrast, blockade of D2Rs with raclopride

(0.2 mg/kg ip) (*22*) did not change the effects produced by L-DOPA (Fig. 1B). These results were confirmed by immunofluorescence analysis of S6 phosphorylated at Ser[240/244] and Ser[235/236] (Fig. 1, C and D) and indicated a prominent role of D1Rs in the ability of L-DOPA to activate mTOR signaling in PD.

D1Rs and D2Rs are present in distinct populations of striatal MSNs, which project, directly or indirectly, respectively, to the output structures of the basal ganglia (*21*). We used transgenic mice expressing enhanced green fluorescent protein (EGFP) under the control of the promoter for the D1R (*Drd1a*-EGFP mice) or the D2R (*Drd2*-EGFP mice) (*23*) to identify the specific subset of MSNs in which L-DOPA regulates S6 phosphorylation.

Fig. 2. L-DOPA activates mTOR signaling in striatonigral MSNs. (**A** and **B**) Immunofluorescence for P-Ser$^{240/244}$-S6 (A) or P-Ser$^{235/236}$-S6 (B) (red), EGFP (green), and DARPP-32 (blue) in the striata of 6-OHDA–lesioned *Drd1a*-EGFP (top) or *Drd2*-EGFP mice (bottom) treated with L-DOPA. Scale bar, 40 μm. (**C** and **D**) Quantification of P-Ser$^{240/244}$-S6 (C) or P-Ser$^{235/236}$-S6 (D) positive cells among EGFP-positive (D1+ or D2+) and EGFP-negative (D1– or D2–) neurons in the dorsal striata of Sham and 6-OHDA–lesioned *Drd1a*- (top) and *Drd2*-EGFP mice (bottom) after administration of L-DOPA. Error bars represent SEM (*n* = 4 mice per treatment). Statistical significance was determined by two-way ANOVA followed by the Bonferroni–Dunn test. ***$P <$ 0.001 versus respective Sham treated with saline.
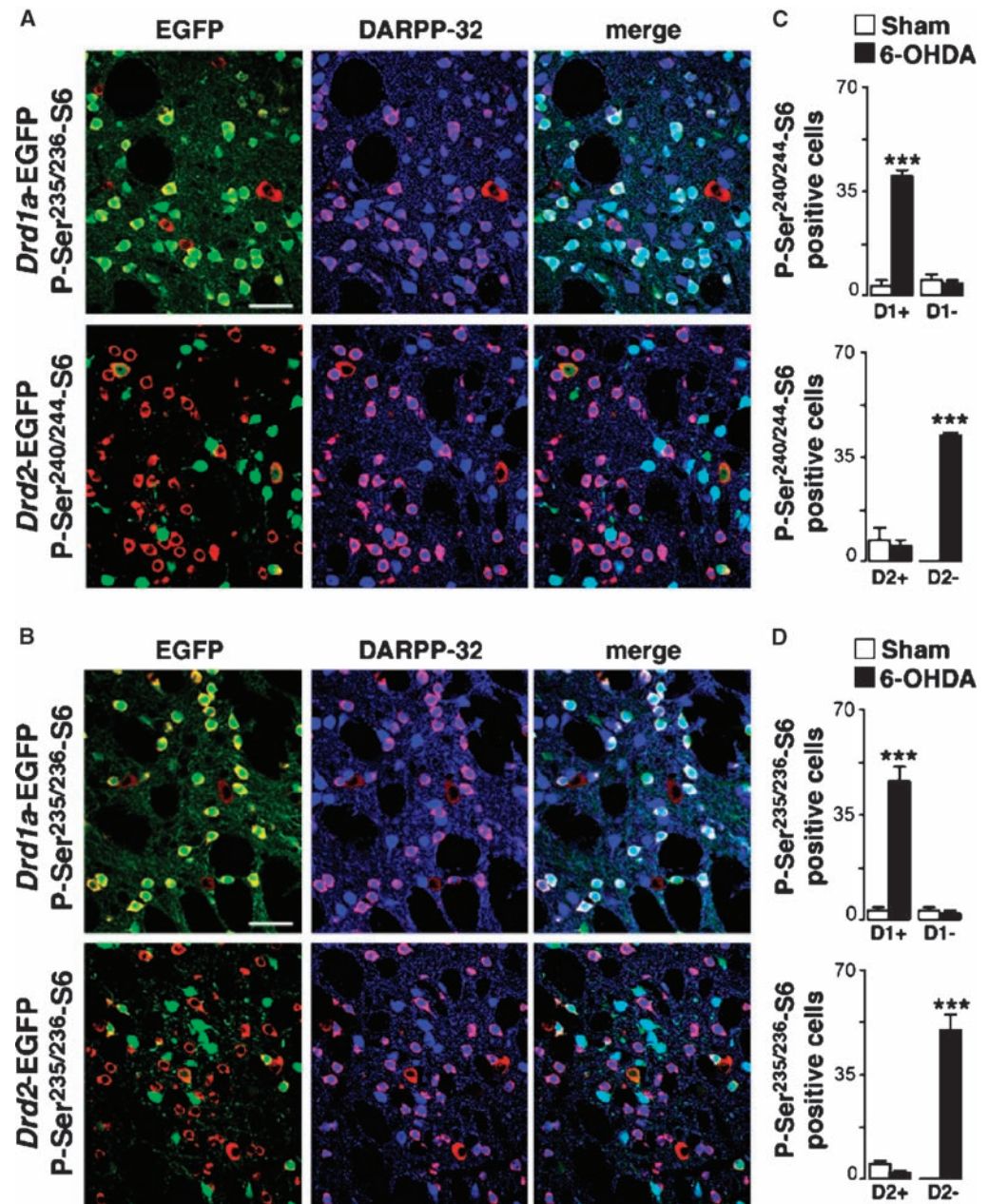
In *Drd1a*-EGFP mice, administration of L-DOPA increased S6 phosphorylation at Ser$^{240/244}$ and Ser$^{235/236}$ mainly in EGFP-positive MSNs (which corresponded to D1R-containing projection neurons) (Fig. 2). Immunoreactivity for phospho-S6 was also detected in a few EGFP-negative cells (Fig. 2, A and B, upper panels). Some of these cells were positive for DARPP-32 [dopamine- and adenosine 3′,5′-monophosphate (cAMP)–regulated phosphoprotein, 32 kD] and corresponded to striatopallidal MSNs, whereas others were devoid of DARPP-32 and most likely represented aspiny cholinergic interneurons (which do not contain D1Rs). In both types of cells, S6 phosphorylation was not affected by administration of L-DOPA (Fig. 2, C and D). In *Drd2*-EGFP mice, L-DOPA produced an increase in immunoreactivity corresponding to S6 phosphorylated at Ser$^{240/244}$ and Ser$^{235/236}$, which was confined to EGFP-negative cells

(Fig. 2, A and B, lower panels). This effect was seen in MSNs, as shown by the presence of DARPP-32 in neurons positive for phospho-Ser$^{240/244}$-S6 and phospho-Ser$^{235/236}$-S6 (Fig. 2, A and B). Together with the pharmacological studies, these results indicate that in 6-OHDA–lesioned mice, L-DOPA activates mTOR signaling in a discrete group of striatal neurons corresponding to the D1R-containing MSNs of the direct pathway.

L-DOPA induces D1R-mediated phosphorylation of 4E-binding protein

We next examined the effect of L-DOPA on the phosphorylation of the eukaryotic translation initiation factor (eIF) 4E-binding protein (4E-BP), which is another major target of mTORC1 (*24*). Lesion with 6-OHDA or administration of L-DOPA did not change the amounts of total or phos-
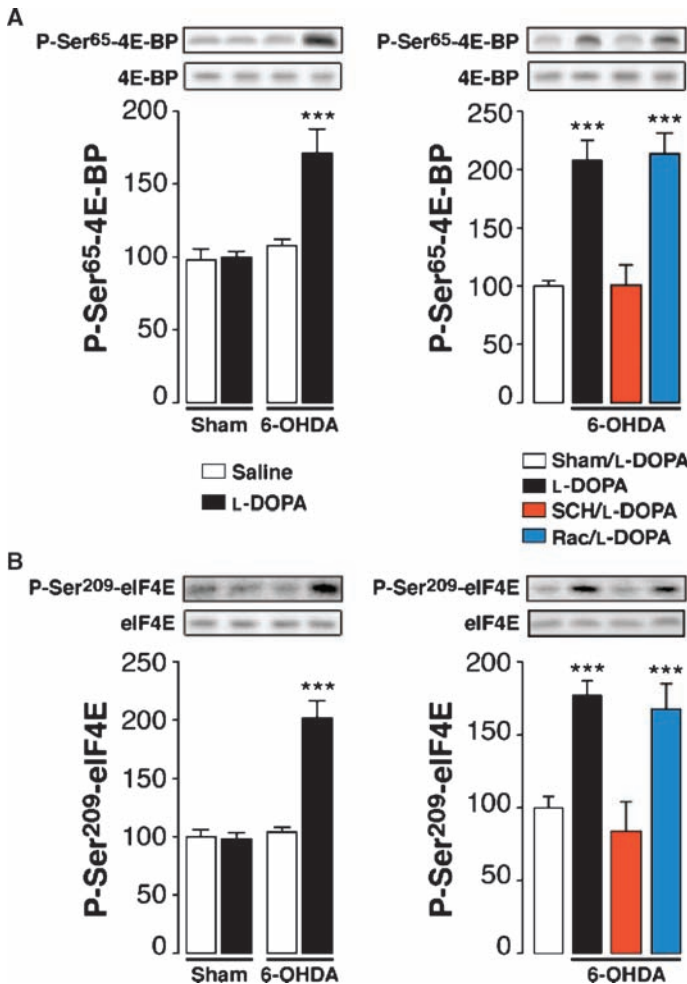
Fig. 3. L-DOPA regulates 4E-BP and eIF4E in 6-OHDA–lesioned mice. (**A** and **B**) Quantification of P-Ser[65]-4E-BP (A) and P-Ser[209]-eIF4E (B) in sham-lesioned mice (Sham) or 6-OHDA–lesioned mice treated with L-DOPA alone or in combination with SCH23390 (SCH) or raclopride (Rac). Representative Western blots of phosphorylated and total proteins are shown (top). Error bars represent SEM (left, *n* = 12 to 24 mice per treatment; right, *n* = 7 to 14 mice per treatment); data were calculated as percent of Sham treated with saline. Statistical significance was determined by two-way (left) and one-way ANOVA (right) followed by the Bonferroni–Dunn test. ***P < 0.001 versus Sham treated with saline.

phorylated 4E-BP (Fig. 3A). However, when combined, these treatments produced a large increase in phospho-Ser[65]-4E-BP without affecting total protein abundance. Moreover, the increase in 4E-BP phosphorylation was prevented by systemic administration of SCH23390, but not of raclopride (Fig. 3A).

L-DOPA increases MAPK interacting kinase–dependent phosphorylation of eukaryotic initiation factor 4E

mTOR-catalyzed phosphorylation of 4E-BP abrogates binding to eukaryotic initiation factor 4E (eIF4E) and leads to the formation of the eIF4F′ multiprotein complex composed of eIF4E, eIF4G, and eIF4A. The assembly of eIF4F′ is the major rate-limiting step in initiation of translation

and is thought to promote phosphorylation of eIF4E on Ser[209] by the MAPK interacting kinases (Mnks) (*25*), which are phosphorylated and activated by ERK (*26*). In 6-OHDA–lesioned mice, treatment with L-DOPA increased phosphorylation of Mnks at Thr[197] and Thr[202] (phospho-Thr[197/202]-Mnks) by 62 ± 8% compared to that of vehicle-treated mice (table S1). This effect was accompanied by a concomitant increase in the phosphorylation of eIF4E, which was prevented by administration of the D1R antagonist SCH23390 (Fig. 3B).

ERK is involved in L-DOPA–mediated activation of mTORC1

ERK-mediated phosphorylation of the guanosine triphosphatase–activating protein, tuberous sclerosis complex 2 (TSC2) (*27*, *28*), is thought to stimulate the small heterotrimeric GTP (guanosine 5′-triphosphate)–binding protein Rheb, which activates mTOR (*29*). It has been reported that ERK stimulates mTORC1 through activation of the p90 ribosomal S6K and phosphorylation of Raptor (*30*). Thus, we tested the involvement of ERK in L-DOPA–mediated activation of mTORC1. Striatal slices from 6-OHDA–lesioned mice were incubated with the D1R agonist SKF81297 (1 μM) in the presence or absence of the MAPK kinase (MEK) inhibitor, U0126 (25 μM). SKF81297 increased the phosphorylation of both S6 (Fig. 4A) and 4E-BP (Fig. 4B), confirming the critical role played by D1Rs in L-DOPA–induced activation of mTORC1 signaling. This effect was paralleled by increased phosphorylation of ERK2, which was blocked by U0126 (Fig. 4C). The MEK inhibitor also prevented SKF81297-induced phosphorylation of S6 and 4E-BP (Fig. 4, A and B) without affecting cAMP-mediated phosphorylation of the glutamate receptor 1 (GluR1) subunit of the AMPA (α-amino-3-hydroxyl-5-methyl-4-isoxazole-propionate)-type glutamate receptor at Ser[845] (Fig. 4D). The notion that ERK plays a critical role in promoting dopamine-dependent mTORC1 signaling was supported by immunostaining showing colocalization of phosphorylated ERK and S6 in striatal MSNs after short-term administration of L-DOPA (Fig. 4E).

Activation of mTORC1 signaling is associated with LID

The results of the biochemical experiments suggested that, during PD, short-term administration of L-DOPA results in the activation of multiple targets of mTOR and in the formation of the eIF4F′ complex, the latter of which is the critical step involved in the regulation of cap-dependent translation. Increased translational efficiency may be involved in long-term adaptive responses to L-DOPA, such as the development of dyskinesia.

To test the possibility that enhanced mTORC1 signaling was associated with dyskinesia, 6-OHDA–lesioned mice were injected for 9 days with L-DOPA (20 mg/kg, one injection per day) in combination with benserazide (12 mg/kg), a procedure that induces dyskinesia (*17*). LID was evaluated by scoring four types of AIMs immediately after the last injection of L-DOPA (*17*). At each time point, the scores for all four types of AIMs were totaled, and the average score was 25.0 ± 0.5 (over a possible range of 0 to 96, with lower scores indicating lower degrees of dyskinesia). The following day, the mice were killed 30 min after L-DOPA administration and striatal tissue was analyzed by Western blotting and immunohistochemistry. Simple regression analysis showed a significant correlation between the severity of AIMs and L-DOPA–induced phosphorylation of S6K and S6 (Fig. 5, A and B). These data were confirmed by immunofluorescence analyses performed in *Drd2*-EGFP mice, in which severely dyskinetic mice showed higher phospho-Ser[240/244]-S6 immunoreactivity in EGFP-negative cells (corresponding to D1R-positive MSNs) compared to sham-lesioned mice or to mice showing low dyskinesia (Fig. 5E). There was also a significant correlation between AIMs and L-DOPA–induced phosphorylation of 4E-BP and eIF4E (Fig. 5, C and D). Thus, activation of mTORC1 in striatal MSNs is present after chronic administration of L-DOPA and correlates with the
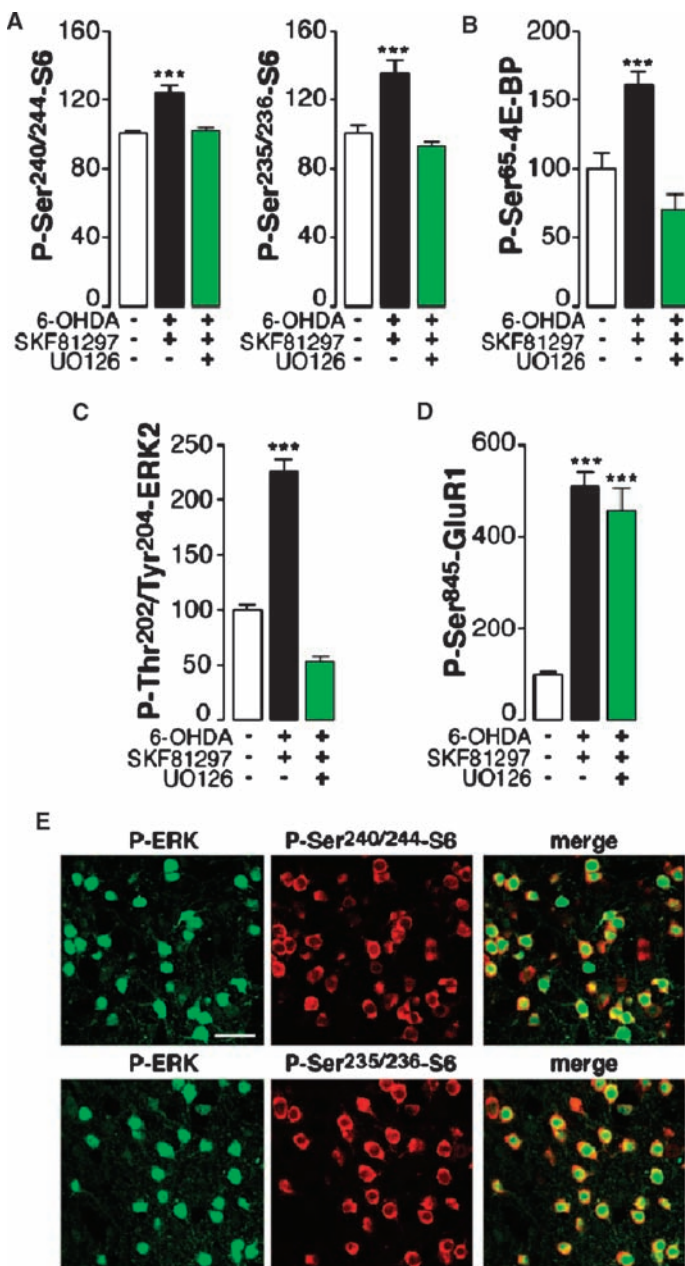
Fig. 4. D1R-mediated activation of mTOR signaling depends on ERK phosphorylation. (**A** to **D**) Striatal slices from sham- and 6-OHDA–lesioned mice were incubated with the D1R agonist SKF81297 (1 μM) for 5 min in the absence or presence of the MEK inhibitor U0126 (25 μM, applied 15 min before SKF81297). Error bars represent SEM, $n = 4$ to 6 pairs of slices per treatment; data were calculated as percent of control (for example, slices from sham-lesioned mice incubated in the absence of drugs). Phosphorylation of S6 (A), 4E-BP (B), and ERK (C) decreased in parallel. In contrast, U0126 did not affect SKF81297-induced phosphorylation of GluR1 at Ser[845], a site regulated by cAMP-dependent protein kinase (D). Statistical significance was determined by one-way ANOVA followed by the Bonferroni–Dunn test. ***$P < 0.001$ versus control. (**E**) Immunostaining for P-ERK and P-Ser[240/244]-S6 (top) or P-Ser[235/236]-S6 (bottom) in the dorsal striatum of a 6-OHDA–lesioned mouse treated with L-DOPA. Scale bar, 40 μm.

severity of AIMs, raising the possibility that the mTORC1 cascade is involved in the development of dyskinesia. Therefore, we examined the effect of rapamycin, the prototypical mTORC1 inhibitor, on AIMs.

Administration of rapamycin reduces LID

Mice lesioned with 6-OHDA were treated for 9 days with L-DOPA (10 mg/kg) in combination with benserazide (7.5 mg/kg) in the absence or presence of rapamycin (2 and 5 mg/kg). Treatment with L-DOPA (10 mg/kg) increased phosphorylation of S6K, S6, 4E-BP, and eIF4E (Fig. 6A). Rapamycin prevented these increases (Fig. 6A) without affecting cAMP or ERK signaling (fig. S1). On day 10, both groups of mice were treated with L-DOPA alone and were scored for AIMs. Mice that had received only L-DOPA plus vehicle during the chronic treatment displayed a robust dyskinetic response. The average score of total AIMs in this experimental group was $19.8 ± 3.5$. In contrast, in mice treated with L-DOPA plus rapamycin (2 or 5 mg/kg), the average score of total AIMs was reduced to $7.0 ± 2.2$ and $6.0 ± 0.7$, respectively (Fig. 6B). In this group of animals, administration of rapamycin in combination with L-DOPA on the day of the test did not produce any additional decrease of dyskinesia; the average score of total AIMs was $7.0 ± 2.6$ and $6.3 ± 1.1$ in mice treated with L-DOPA plus rapamycin (2 and 5 mg/kg, respectively). These data indicated that blockade of mTORC1 signaling reduced the development of dyskinesia produced by chronic administration of L-DOPA.

The ability of rapamycin to counteract the action of L-DOPA might have affected the anti-Parkinsonian properties of this drug. We examined this possibility by comparing the effect of combined administration of L-DOPA plus rapamycin with that of L-DOPA plus vehicle in the cylinder test. Rapamycin did not diminish the efficacy of L-DOPA to counteract forelimb akinesia produced by the 6-OHDA lesion (Fig. 6C). Therefore, blockade of mTORC1 signaling does not appear to affect the therapeutic (anti-akinetic) action of L-DOPA.

DISCUSSION

Here, we show that, in a mouse model of PD, administration of L-DOPA activated mTORC1 signaling in a well-defined population of striatal projection MSNs belonging to the direct pathway. This effect was exerted through activation of D1Rs and represents, to the best of our knowledge, the first connection between dopaminergic transmission and mTOR signaling in the striatum. In addition, persistent activation of the mTORC1 cascade during chronic administration of L-DOPA was associated with the development of dyskinesia and administration of the mTORC1 inhibitor rapamycin reduced dyskinesia.

In the striatum, loss of dopaminergic innervation results in the development of a sensitization to D1R agonists, which has been implicated in the development of LID (2–4). We showed that the ability of L-DOPA to activate mTORC1 signaling was due to this hypersensitivity of D1Rs. Thus, the increases in phosphorylation of S6K, S6, and 4E-BP that were caused by administration of L-DOPA to 6-OHDA–lesioned mice were blocked by a D1R antagonist. Moreover, the L-DOPA–induced increase in S6 phosphorylation was localized to the MSNs of the direct, striatonigral pathway, which contain D1Rs but not D2Rs (21, 23).

It has been reported that the substantia nigra of PD patients and of mice treated with the dopaminergic toxin, 1-methyl-4-phenyl-1,2,3,6-tetrahydropyridine, contains higher amounts of the stress-regulated protein RTP801 (31, 32), which is an mTOR inhibitor (33, 34). We did not examine the effect of 6-OHDA on the abundance of RTP801; however, 6-OHDA did not modify basal mTORC1 activity in striatal MSNs, as indicated by unchanged amounts of phosphorylated downstream targets. Moreover, in striatal MSNs, 6-OHDA promoted L-DOPA–induced activation
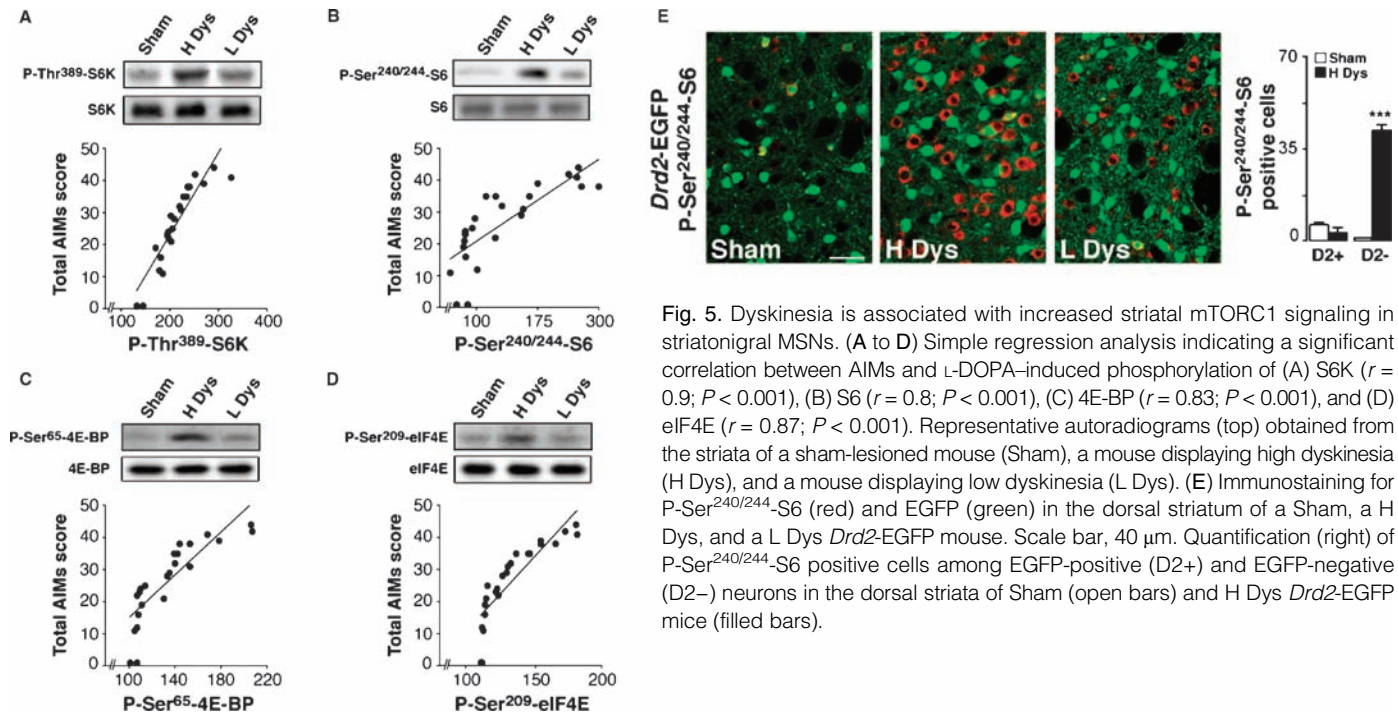
Fig. 5. Dyskinesia is associated with increased striatal mTORC1 signaling in striatonigral MSNs. (**A** to **D**) Simple regression analysis indicating a significant correlation between AIMs and L-DOPA–induced phosphorylation of (A) S6K ($r = 0.9$; $P < 0.001$), (B) S6 ($r = 0.8$; $P < 0.001$), (C) 4E-BP ($r = 0.83$; $P < 0.001$), and (D) eIF4E ($r = 0.87$; $P < 0.001$). Representative autoradiograms (top) obtained from the striata of a sham-lesioned mouse (Sham), a mouse displaying high dyskinesia (H Dys), and a mouse displaying low dyskinesia (L Dys). (**E**) Immunostaining for P-Ser$^{240/244}$-S6 (red) and EGFP (green) in the dorsal striatum of a Sham, a H Dys, and a L Dys *Drd2*-EGFP mouse. Scale bar, 40 μm. Quantification (right) of P-Ser$^{240/244}$-S6 positive cells among EGFP-positive (D2+) and EGFP-negative (D2−) neurons in the dorsal striata of Sham (open bars) and H Dys *Drd2*-EGFP mice (filled bars).

of mTORC1. Therefore, increased RTP801 or its negative effect on mTOR signaling appears to be limited to midbrain dopaminergic neurons.

Our data show that repeated administration of L-DOPA led to a normalization of sensitized mTORC1 signaling. However, such normalization occurred only in mice with undetectable or low dyskinesia, whereas in highly dyskinetic mice, the ability of L-DOPA to activate mTORC1 was fully preserved (Fig. 5 and table S1). Thus, LID was associated with persistent enhancement of mTORC1 signaling, which appears to result from the inability of the MSNs of the direct pathway to normalize their response to L-DOPA during the course of chronic administration. An identical pattern of regulation with respect to L-DOPA–induced activation of ERK has been described in 6-OHDA–lesioned mice and rats (*4*, *8*, *35*). In the mouse, ERK phosphorylation in response to L-DOPA occurs in the MSNs of the direct pathway (*35*), that is, in the same group of neurons in which mTORC1 signaling is increased. In agreement with this finding, we found almost complete colocalization in striatal neurons between L-DOPA–induced phospho-ERK and phospho-S6. Furthermore, blockade of ERK, achieved with the MEK inhibitor U0126, prevented the ability of a D1R agonist to phosphorylate S6 and 4E-BP. Together, these observations indicate that activation of ERK is implicated in the increase in mTORC1 signaling produced by L-DOPA in dyskinetic mice. This regulation may be exerted by ERK through inhibition of TSC2 and sequential activation of Rheb and mTOR (*27*, *28*) or through phosphorylation and activation of the mTORC1 component, Raptor (*30*).

The ability of ERK to promote mTORC1 signaling in striatal MSNs is further supported by the observation that administration of L-DOPA, as well as dyskinesia, was accompanied by increased phosphorylation of Mnks (table S1), which are direct targets of ERK (*26*). Mnks bind to eIF4G and catalyze the phosphorylation of eIF4E (*25*). In line with this notion, we found increased amounts of phosphorylated eIF4E in the striata of dyskinetic mice. Although the role of eIF4E phosphorylation remains to be fully understood (*36*), this event has been proposed to occur during the cap-dependent initiation process (*37*). Thus, the increase in eIF4E

phosphorylation associated with LID may reflect increased formation of the initiation complex eIF4F′. In support of this idea, we found that inhibition of mTORC1 by rapamycin, which prevents phosphorylation of 4E-BP, thereby promoting the sequestration of eIF4E and reducing the formation of eIF4F′, leads to concomitant abolishment of L-DOPA–induced eIF4E phosphorylation.

The observation that abnormal phosphorylation of several components of the mTORC1 signaling cascade correlates with the severity of LID raises the question of the possible antidyskinetic effects produced by suppression of mTORC1 signaling. Previous studies have shown that blockade of ERK, which is required for mTORC1 signaling, attenuates dyskinetic behavior in mice and rats (*7*, *10*). However, because of the involvement of ERK in basic physiological processes, including transcriptional regulation, ERK inhibitors in the treatment of dyskinesia are not likely to be used clinically. In this regard, one key finding of this study is that LID was reduced by inhibiting mTORC1, which is located downstream of ERK and is not involved in ERK-mediated transcriptional control. Indeed, administration of rapamycin counteracts LID without interfering with the regulation of nuclear targets of ERK, such as histone H3, which is highly phosphorylated in LID (*7*, *35*) (fig. S2). Rapamycin and its derivatives are currently tested in humans as anticancer therapeutics (*38*). The present data suggest that these drugs and other classes of mTORC1 inhibitors are potential antidyskinetic agents for the treatment of PD.

In conclusion, this study implicates mTORC1 signaling in dopaminergic transmission in the MSNs of the direct, striatonigral pathway. Moreover, suppression of mTORC1 signaling in this neuronal population is paralleled by a reduction of dyskinesia caused by L-DOPA. It is possible that abnormal activation of the mTORC1 signaling machinery during chronic administration of L-DOPA results in changes in mRNA translation and protein production. These changes may be involved, for instance, in dysfunctions of long-term potentiation or depotentiation at corticostriatal synapses, which have been associated with PD and LID (*14*). Further studies will be necessary to assess the role played by mTORC1 signaling in striatal transmission and plasticity.

Fig. 6. Inhibition of mTOR signaling reduces dyskinesia without affecting the anti-akinetic properties of ʟ-DOPA. (**A**) Rapamycin prevents ʟ-DOPA–induced phosphorylation of S6K, S6, 4E-BP, and eIF4E. Representative Western blotting of phosphorylated and total proteins is shown (top). Error bars in graphs represent SEM (n = 8 to 16 mice per treatment) of data calculated as percent of Sham treated with ʟ-DOPA. Statistical significance was determined by one-way ANOVA followed by the Bonferroni–Dunn test. ***$P < 0.001$ versus Sham treated with ʟ-DOPA. °°$P < 0.01$ and °°°$P < 0.001$ versus 6-OHDA–lesioned mice treated with ʟ-DOPA. (**B**) Time profile of total axial, limb, orolingual, and locomotive AIMs scored every 20 min over a period of 120 min after the last drug administration (left). Sum of total AIMs scored during all observation periods (right). Statistical significance was determined by one-way ANOVA followed by the Bonferroni–Dunn test. ***$P < 0.001$ versus mice treated chronically with ʟ-DOPA plus vehicle (Veh). (**C**) Left forelimb use determined by the cylinder test in 6-OHDA–lesioned mice before (left) and after (right) administration of ʟ-DOPA plus vehicle or rapamycin (2 and 5 mg/kg). Broken line shows the percent of left forelimb use determined in sham-lesioned mice (47 ± 3). Statistical significance was determined by repeated-measures ANOVA. ***$P < 0.001$ versus untreated 6-OHDA–lesioned mice.
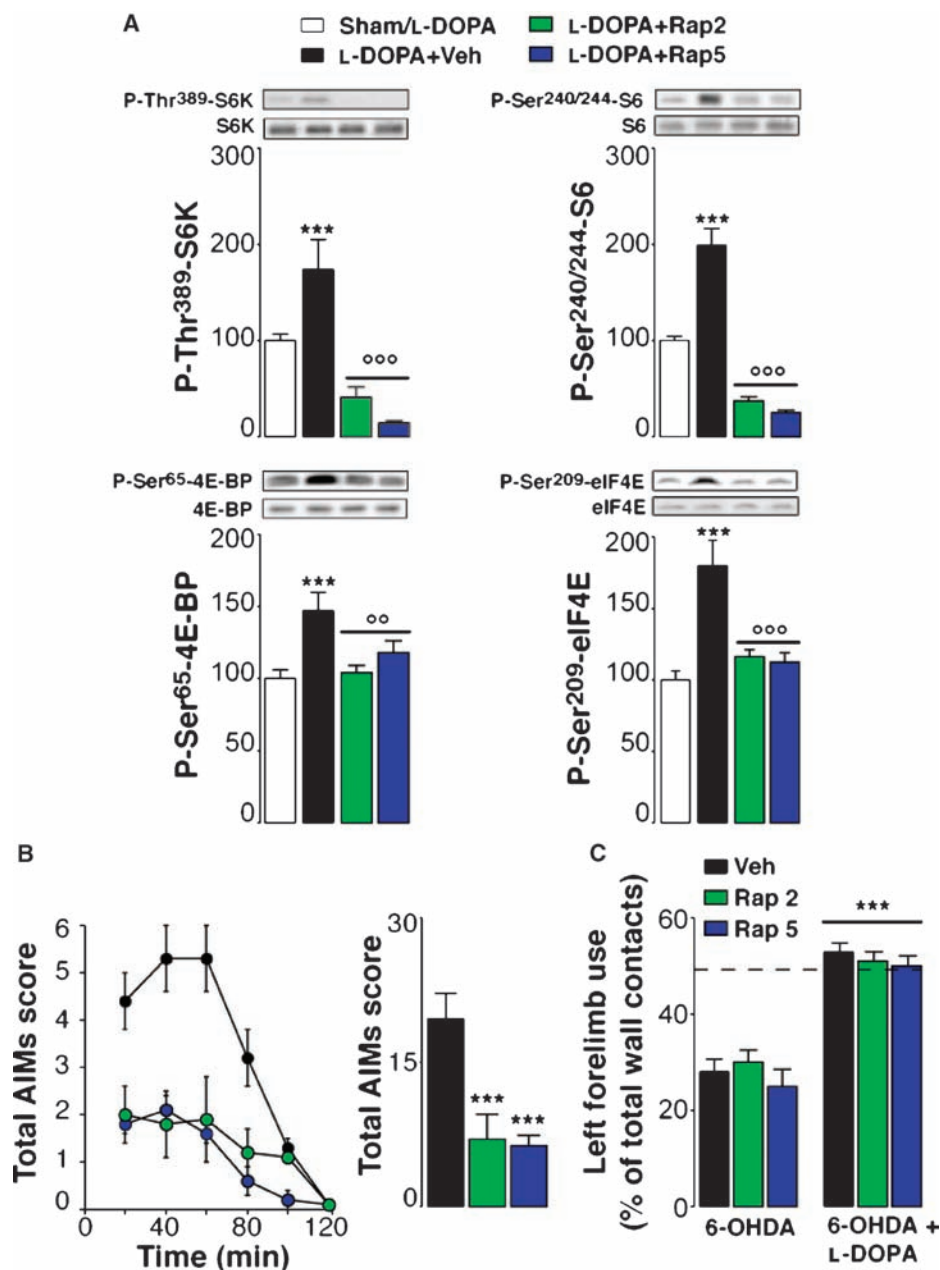
MATERIALS AND METHODS

Animals

Male C57BL/6J mice (30 g) were purchased from Taconic (Tornbjerg, Denmark). Bacterial artificial chromosome transgenic mice expressing EGFP under the control of the promoter for D2R (*Drd2*-EGFP) or D1R (*Drd1a*-EGFP) were generated by the GENSAT (Gene Expression Nervous System Atlas) program at the Rockefeller University (*23*) and were crossed on a C57BL/6 background for three generations. The animals were housed in groups of five under standardized conditions with a 12-hour light-dark cycle and stable temperature (20°C) and humidity (40 to 50%).

Drugs

All drugs, with the exception of rapamycin (see below), were purchased from Sigma-Aldrich Sweden AB (Stockholm), dissolved in saline (0.9% NaCl), and injected intraperitoneally in a volume of 10 ml per kilogram of body weight. ʟ-DOPA was injected at a dose of 10 or 20 mg/kg in combination with the peripheral DOPA decarboxylase inhibitor, benserazide hydrochloride (7.5 or 12 mg/kg). SCH23390 (0.125 mg/kg) and raclopride (0.2 mg/kg) were administered 10 min before administration of ʟ-DOPA. The doses of SCH23390 and raclopride were chosen on the basis of previous studies in C57BL/6 mice showing their ability to effectively antagonize D1Rs and D2Rs, respectively (*22, 35, 39*). Rapamycin (2 and 5 mg/kg) (LC Laboratories, Woburn, MA) was dissolved in a solution of 5% dimethyl

sulfoxide (DMSO), 15% PEG-400 (polyethylene glycol, molecular weight 400), and 5% Tween-20 and was administered once per day in a volume of 2 ml per kilogram body weight, starting 3 days before the beginning of the treatment with L-DOPA. For the combined treatment, rapamycin was injected 1 hour before administration of L-DOPA. Mice that did not receive rapamycin were injected with an equivalent amount of vehicle (5% DMSO, 15% PEG-400, and 5% Tween-20). This treatment did not produce any adverse effect or any change in the intensity of LID, even when repeated over 10 days; the average scores for total AIMs were 19.5 ± 0.5 for mice treated with L-DOPA plus vehicle and 18.0 ± 5.8 for mice treated with L-DOPA without vehicle. For the experiments on slices, SKF81297 (1 μM) and U0126 (25 μM) (Sigma-Aldrich Sweden AB, Stockholm) were dissolved in saline and DMSO, respectively, and diluted 1:100 in incubation buffer.

6-OHDA lesioning

Mice were anesthetized with a mixture of fentanyl citrate (0.315 mg/ml), fluanisone (10 mg/ml) (VetaPharma, Leeds, UK), midazolam (5 mg/ml) (Hameln Pharmaceuticals, Gloucester, UK), and water (1:1:2 in a volume of 10 ml/kg) and mounted in a stereotaxic frame (David Kopf Instruments, Tujunga, CA) equipped with a mouse adaptor. 6-OHDA-HCl (Sigma-Aldrich Sweden AB) was dissolved in 0.02% ascorbic acid in saline at a concentration of 3 μg of free base 6-OHDA per microliter. Each mouse received two unilateral injections of 6-OHDA (2 μl per injection) into the right striatum as previously described (7), according to the following coordinates (mm) (40): anteroposterior (AP), +1; mediolateral (ML), −2.1; dorsoventral (DV), −3.2; and AP +0.3; ML, −2.3; DV, −3.2. Animals were allowed to recover for 3 weeks before behavioral evaluation and drug treatment were carried out. This procedure leads to ≥80% decrease in striatal tyrosine hydroxylase immunoreactivity. The efficacy of the lesion is illustrated by the loss of tyrosine hydroxylase immunoreactivity in both striatum and substantia nigra pars compacta (fig. S3).

Cylinder test

The cylinder test (41) was used to monitor the anti-akinetic effect of L-DOPA. Mice were placed in individual glass cylinders (diameter, 12 cm) and movements were recorded for 5 min. Each 6-OHDA–lesioned mouse was tested before L-DOPA treatment and 1 hour after the first injection of L-DOPA or L-DOPA plus rapamycin (2 and 5 mg/kg). The number of contacts of either forelimb with the wall was counted by an observer blind to the mouse treatment. To discriminate between accidental touches and meaningful physiological movements, only wall contacts where the animal supported its body weight on the paw with extended digits were counted. The use of the impaired (left) forelimb was calculated as a percentage of the total number of supporting wall contacts. Sham-lesioned mice, which showed $47 \pm 3\%$ (broken line in Fig. 6C) left forelimb use, were used as control.

Abnormal involuntary movements

6-OHDA–lesioned mice were treated for 9 days with one injection per day of L-DOPA (20 or 10 mg/kg) plus benserazide (12 or 7.5 mg/kg). The effect of rapamycin was examined by treating 6-OHDA–lesioned mice for 9 days with L-DOPA–benserazide plus rapamycin (2 and 5 mg/kg) and, on day 10, by administering L-DOPA in combination with vehicle or rapamycin. AIMs were assessed with a pharmacologically validated mouse model of LID after the last injection of L-DOPA (day 10) by an observer blind to the mouse treatment (17). Briefly, 20 min after L-DOPA administration, mice were placed in separate cages and individual dyskinetic behaviors were assessed for a 1-min monitoring period every 20 min, over a period of 120 min. Purposeless movements, distinguished from natural stereotyped behaviors (such as grooming, sniffing, rearing, and gnawing), were classified into four

subtypes: locomotive AIMs (tight contralateral turns), axial AIMs (contralateral dystonic posture of the neck and upper body toward the side contralateral to the lesion), limb AIMs (jerky and fluttering movements of the limb contralateral to the side of the lesion), and orolingual AIMs (vacuous jaw movements and tongue protrusions). Each subtype was scored on a severity scale from 0 to 4: 0, absent; 1, occasional; 2, frequent; 3, continuous; and 4, continuous and not interruptible by outer stimuli.

In vitro experiments

Sham- or 6-OHDA–lesioned mice were killed by decapitation and the brains were rapidly removed. Coronal slices (250 μm) were prepared with the use of a vibratome (Leica, Nussloch, Germany). Dorsal striata were dissected out from each slice under a microscope. Two slices were placed in individual 5-ml polypropylene tubes containing 2 ml of Krebs-Ringer bicarbonate buffer [KRB; 118 mM NaCl, 4.7 mM KCl, 1.3 mM CaCl₂, 1.5 mM MgSO₄, 1.2 mM KH₂PO₄, 25 mM NaHCO₃, and 11.7 mM glucose equilibrated with 95% O_2–5% CO_2 (v/v) (pH 7)]. The samples were equilibrated at 30°C for two 30-min intervals, each followed by replacement of the medium with 2 ml of fresh KRB. Slices were first incubated for 15 min in the presence of U0126 or vehicle and then for 5 min in the presence of SKF81297 (1 μM). After incubation, the solutions were rapidly removed, the slices were sonicated in 1% SDS, and the samples were analyzed by Western blotting as described below.

In vivo experiments

Mice were treated with L-DOPA and benserazide alone or in combination with SCH23390, raclopride, or rapamycin and killed by decapitation 30 min later. The heads of the animals were cooled in liquid nitrogen for 6 s and the brains were removed. The striata were dissected out on an ice-cold surface, sonicated in 750 μl of 1% SDS, and boiled for 10 min. The effectiveness of this extraction procedure in preventing protein phosphorylation and dephosphorylation, hence ensuring that the state of phosphorylation of phosphoproteins measured ex vivo reflects the in vivo situation, has previously been shown (39).

Western blotting

Aliquots (5 μl) of the homogenate were used for protein determination with a BCA (bicinchoninic acid) assay kit (Pierce Europe, Oud Beijerland, the Netherlands). Equal amounts of protein (30 μg) for each sample were loaded onto 10% polyacrylamide gels. Proteins were separated by SDS–polyacrylamide gel electrophoresis and transferred overnight to polyvinylidene difluoride membranes (Amersham Pharmacia Biotech, Uppsala, Sweden) (42). The membranes were immunoblotted with antibodies against phospho-Thr^{389}-S6K (1:1000), S6K dually phosphorylated at Thr$^{421/424}$ (1:1000), S6 dually phosphorylated at Ser$^{240/244}$-S6 (1:1000), or Ser$^{235/236}$-S6 (1:1000), phospho-Ser^{65}-4E-BP (1:1000), Mnks dually phosphorylated at phospho-Thr$^{197/202}$, phospho-Ser^{209}-eIF4E (1:1000), ERK1-2 dually phosphorylated at Thr^{202} and Tyr^{204} (1:2000) (Cell Signaling Technology, Beverly, MA), and phospho-Ser^{845}-GluR1 (PhosphoSolutions, Aurora, CO) (1:750). Antibodies against S6, S6K, 4E-BP, Mnks, eIF4E, ERK, and GluR1 (1:1000, Cell Signaling Technology) that are not phosphorylation state–specific were used to estimate the total amount of proteins. An antibody against tyrosine hydroxylase (1:1000, Chemicon International, Temecula, CA) was used to assess the severity of 6-OHDA lesions. Detection was based on fluorescent secondary antibody binding and quantified with a Li-Cor Odyssey infrared fluorescent detection system (Li-Cor, Lincoln, NE). The amount of each phosphoprotein was normalized for the amount of the corresponding total protein detected in the sample.

Tissue preparation and immunofluorescence

Mice were rapidly anaesthetized with pentobarbital (100 mg/kg ip, Sanofi-Aventis, France) and perfused transcardially with 4% (w/v) paraformaldehyde in 0.1 M sodium phosphate buffer (pH 7.5). Brains were postfixed overnight in the same solution and stored at 4°C. Thirty-micrometer-thick sections were cut with a vibratome (Leica, Nussloch, Germany) and stored at −20°C in 0.1 M sodium phosphate buffer containing 30% (v/v) ethylene glycol and 30% (v/v) glycerol until they were processed for immunofluorescence. Free-floating sections were rinsed in tris-buffered saline [TBS; 0.25 M tris and 0.5 M NaCl (pH 7.5)], incubated for 5 min in TBS containing 3% H_2O_2 and 10% methanol (v/v), and then rinsed three times for 10 min each in TBS. After 20 min of incubation in 0.2% Triton X-100 in TBS, sections were again rinsed three times in TBS. Finally, they were incubated overnight at 4°C with the different primary antibodies. For detection of phosphorylated proteins, 0.1 mM NaF was included in all buffers and incubation solutions. Phosphorylation was analyzed with rabbit polyclonal antibodies that recognize histone H3 only when acetylated on Lys^{14} and phosphorylated at Ser^{10}, and S6 only when dually phosphorylated at $Ser^{240/244}$ or $Ser^{235/236}$ (1:500, Cell Signaling Technology). In the double-labeling experiments, a monoclonal antibody against EGFP (1:500, Invitrogen) was used to detect EGFP fluorescence in *Drd2*- and *Drd1a*-EGFP mice. A mouse monoclonal antibody against diphospho-Thr^{202}/Tyr^{204}-ERK1/2 (1:400, Sigma-Aldrich Sweden AB) was used for some double-labeling experiments. In the triple-labeling experiments, a monoclonal antibody against DARPP-32 (1:1000) was used (*43*). After incubation with primary antibodies, sections were rinsed three times for 10 min in TBS and incubated for 45 min with goat secondary antibody against rabbit or Cy3-coupled secondary antibody against mouse (1:400, Jackson Laboratory, Bar Harbor, ME), or goat Alexa Fluor 488– or Alexa Fluor 633–conjugated secondary antibodies against mouse (1:400, Invitrogen AB, Stockholm, Sweden). In the triple-labeling experiment, after incubation with the secondary antibodies, the slices were then rinsed three times for 10 min in TBS and incubated overnight with a polyclonal antibody against EGFP directly coupled to Alexa Fluor 488 (1:500, Invitrogen AB). A monoclonal antibody against tyrosine hydroxylase (1:1000, Chemicon International) was also used to assess the severity of 6-OHDA lesions. Sections were rinsed for 10 min twice in TBS and twice in TB (0.25 M tris) before mounting in 1,4-diazabicyclo-[2. 2. 2]-octane (DABCO, Sigma-Aldrich Sweden AB). Single-, double-, and triple-labeled images from the dorsolateral striatum were obtained by sequential laser scanning confocal microscopy (Zeiss LSM). Neuronal quantification was performed in 562 × 562-μm or 375 × 375-μm images. In all the experiments, phospho-S6 positive cells were only counted when colocalized with DARPP-32- or EGFP-positive neurons for assessment of D2R- or D1R-positive cells.

Statistics

Data were analyzed with one-way or two-way analysis of variance (ANOVA), where treatment and time were the independent variables, followed by Bonferroni–Dunn post hoc test for specific comparisons. Data expressed as percentages were subjected to arcsine square root transformation (p_i = arcsine $\sqrt{p}$) before ANOVA.

SUPPLEMENTARY MATERIALS

www.sciencesignaling.org/cgi/content/full/2/80/ra36/DC1

Fig. S1. Rapamycin does not affect L-DOPA–induced phosphorylation of GluR1 and ERK2.

Fig. S2. Rapamycin does not affect L-DOPA–induced phosphorylation of Lys^{14}-acetylated histone H3.

Fig. S3. Evaluation of the degree of DA denervation after striatal 6-OHDA injection.

Table S1. Effect of 6-OHDA and L-DOPA on selected proteins involved in mTOR signaling.

REFERENCES AND NOTES

1. S. J. Kish, K. Shannak, O. Hornykiewicz, Uneven pattern of dopamine loss in the striatum of patients with idiopathic Parkinson's disease. Pathophysiologic and clinical implications. *N. Engl. J. Med.* **318**, 876–880 (1988).
2. M. A. Cenci, Dopamine dysregulation of movement control in L-DOPA–induced dyskinesia. *Trends Neurosci.* **30**, 236–243 (2007).
3. C. Guigoni, I. Aubert, Q. Li, V. V. Gurevich, J. L. Benovic, S. Ferry, U. Mach, H. Stark, L. Leriche, K. Håkansson, B. H. Bioulac, C. E. Gross, P. Sokoloff, G. Fisone, E. V. Gurevich, B. Bloch, E. Bezard, Pathogenesis of levodopa-induced dyskinesia: Focus on D1 and D3 dopamine receptors. *Parkinsonism Relat. Disord.* **11** (Suppl. 1), S25–S29 (2005).
4. E. Santini, E. Valjent, G. Fisone, Parkinson's disease: Levodopa-induced dyskinesia and signal transduction. *FEBS J.* **275**, 1392–1399 (2008).
5. C. R. Gerfen, S. Miyachi, R. Paletzki, P. Brown, D1 dopamine receptor supersensitivity in the dopamine-depleted striatum results from a switch in the regulation of ERK1/2/MAP kinase. *J. Neurosci.* **22**, 5042–5054 (2002).
6. N. Pavón, A. B. Martín, A. Mendialdua, R. Moratalla, ERK phosphorylation and FosB expression are associated with L-DOPA-induced dyskinesia in hemiparkinsonian mice. *Biol. Psychiatry* **59**, 64–74 (2006).
7. E. Santini, E. Valjent, A. Usiello, M. Carta, A. Borgkvist, J. A. Girault, D. Hervé, P. Greengard, G. Fisone, Critical involvement of cAMP/DARPP-32 and extracellular signal-regulated protein kinase signaling in l-DOPA-induced dyskinesia. *J. Neurosci.* **27**, 6995–7005 (2007).
8. J. E. Westin, L. Vercammen, E. M. Strome, C. Konradi, M. A. Cenci, Spatiotemporal pattern of striatal ERK1/2 phosphorylation in a rat model of L-DOPA-induced dyskinesia and the role of dopamine D1 receptors. *Biol. Psychiatry* **62**, 800–810 (2007).
9. G. M. Thomas, R. L. Huganir, MAPK cascade signalling and synaptic plasticity. *Nat. Rev. Neurosci.* **5**, 173–183 (2004).
10. S. Schuster, A. Nadjar, J. T. Guo, Q. Li, C. Ittrich, B. Hengerer, E. Bezard, The 3-hydroxy-3-methylglutaryl-CoA reductase inhibitor lovastatin reduces severity of L-DOPA-induced abnormal involuntary movements in experimental Parkinson's disease. *J. Neurosci.* **28**, 4311–4316 (2008).
11. M. Costa-Mattioli, W. S. Sossin, E. Klann, N. Sonenberg, Translational control of long-lasting synaptic plasticity and memory. *Neuron* **61**, 10–26 (2009).
12. P. Tsokas, E. A. Grace, P. Chan, T. Ma, S. C. Sealfon, R. Iyengar, E. M. Landau, R. D. Blitzer, Local protein synthesis mediates a rapid increase in dendritic elongation factor 1A after induction of late long-term potentiation. *J. Neurosci.* **25**, 5833–5843 (2005).
13. S. J. Tang, G. Reis, H. Kang, A. C. Gingras, N. Sonenberg, E. M. Schuman, A rapamycin-sensitive signaling pathway contributes to long-term synaptic plasticity in the hippocampus. *Proc. Natl. Acad. Sci. U.S.A.* **99**, 467–472 (2002).
14. B. Picconi, D. Centonze, K. Håkansson, G. Bernardi, P. Greengard, G. Fisone, M. A. Cenci, P. Calabresi, Loss of bidirectional striatal synaptic plasticity in l-DOPA-induced dyskinesia. *Nat. Neurosci.* **6**, 501–506 (2003).
15. D. A. Perese, J. Ulman, J. Viola, S. E. Ewing, K. S. Bankiewicz, A 6-hydroxydopamine-induced selective parkinsonian rat model. *Brain Res.* **494**, 285–293 (1989).
16. U. Ungerstedt, 6-hydroxy-dopamine induced degeneration of central monoamine neurons. *Eur. J. Pharmacol.* **5**, 107–110 (1968).
17. M. Lundblad, A. Usiello, M. Carta, K. Håkansson, G. Fisone, M. A. Cenci, Pharmacological validation of a mouse model of L-DOPA-induced dyskinesia. *Exp. Neurol.* **194**, 66–75 (2005).
18. G. Thomas, M. Siegmann, J. Gordon, Multiple phosphorylation of ribosomal protein S6 during transition of quiescent 3T3 cells into early G1, and cellular compartmentalization of the phosphate donor. *Proc. Natl. Acad. Sci. U.S.A.* **76**, 3952–3956 (1979).
19. N. Pullen, G. Thomas, The modular phosphorylation and activation of p70s6k. *FEBS Lett.* **410**, 78–82 (1997).
20. I. Ruvinsky, O. Meyuhas, Ribosomal protein S6 phosphorylation: From protein synthesis to cell size. *Trends Biochem. Sci.* **31**, 342–348 (2006).
21. C. R. Gerfen, The neostriatal mosaic: Multiple levels of compartmental organization in the basal ganglia. *Annu. Rev. Neurosci.* **15**, 285–320 (1992).
22. J. Bertran-Gonzalez, K. Håkansson, A. Borgkvist, T. Irinopoulou, K. Brami-Cherrier, A. Usiello, P. Greengard, D. Hervé, J. A. Girault, E. Valjent, G. Fisone, Histone H3 phosphorylation is under the opposite tonic control of dopamine D2 and adenosine A2A receptors in striatopallidal neurons. *Neuropsychopharmacology* **34**, 1710–1720 (2009).
23. S. Gong, C. Zheng, M. L. Doughty, K. Losos, N. Didkovsky, U. B. Schambra, N. J. Nowak, A. Joyner, G. Leblanc, M. E. Hatten, N. Heintz, A gene expression atlas of the central nervous system based on bacterial artificial chromosomes. *Nature* **425**, 917–925 (2003).
24. A. C. Gingras, B. Raught, S. P. Gygi, A. Niedzwiecka, M. Miron, S. K. Burley, R. D. Polakiewicz, A. Wysłouch-Cieszynska, R. Aebersold, N. Sonenberg, Hierarchical phosphorylation of the translation inhibitor 4E-BP1. *Genes Dev.* **15**, 2852–2864 (2001).
25. S. Pyronnet, H. Imataka, A. C. Gingras, R. Fukunaga, T. Hunter, N. Sonenberg, Human eukaryotic translation initiation factor 4G (eIF4G) recruits mnk1 to phosphorylate eIF4E. *EMBO J.* **18**, 270–279 (1999).

26. A. J. Waskiewicz, A. Flynn, C. G. Proud, J. A. Cooper, Mitogen-activated protein kinases activate the serine/threonine kinases Mnk1 and Mnk2. *EMBO J.* **16**, 1909–1920 (1997).

27. L. Ma, Z. Chen, H. Erdjument-Bromage, P. Tempst, P. P. Pandolfi, Phosphorylation and functional inactivation of TSC2 by Erk implications for tuberous sclerosis and cancer pathogenesis. *Cell* **121**, 179–193 (2005).

28. P. P. Roux, B. A. Ballif, R. Anjum, S. P. Gygi, J. Blenis, Tumor-promoting phorbol esters and activated Ras inactivate the tuberous sclerosis tumor suppressor complex via p90 ribosomal S6 kinase. *Proc. Natl. Acad. Sci. U.S.A.* **101**, 13489–13494 (2004).

29. X. Long, Y. Lin, S. Ortiz-Vega, K. Yonezawa, J. Avruch, Rheb binds and regulates the mTOR kinase. *Curr. Biol.* **15**, 702–713 (2005).

30. A. Carrière, M. Cargnello, L. A. Julien, H. Gao, E. Bonneil, P. Thibault, P. P. Roux, Oncogenic MAPK signaling stimulates mTORC1 activity by promoting RSK-mediated raptor phosphorylation. *Curr. Biol.* **18**, 1269–1277 (2008).

31. C. Malagelada, Z. H. Jin, L. A. Greene, RTP801 is induced in Parkinson's disease and mediates neuron death by inhibiting Akt phosphorylation/activation. *J. Neurosci.* **28**, 14363–14371 (2008).

32. C. Malagelada, E. J. Ryu, S. C. Biswas, V. Jackson-Lewis, L. A. Greene, RTP801 is elevated in Parkinson brain substantia nigral neurons and mediates death in cellular models of Parkinson's disease by a mechanism involving mammalian target of rapamycin inactivation. *J. Neurosci.* **26**, 9996–10005 (2006).

33. J. Brugarolas, K. Lei, R. L. Hurley, B. D. Manning, J. H. Reiling, E. Hafen, L. A. Witters, L. W. Ellisen, W. G. Kaelin Jr., Regulation of mTOR function in response to hypoxia by REDD1 and the TSC1/TSC2 tumor suppressor complex. *Genes Dev.* **18**, 2893–2904 (2004).

34. M. N. Corradetti, K. Inoki, K. L. Guan, The stress-inducted proteins RTP801 and RTP801L are negative regulators of the mammalian target of rapamycin pathway. *J. Biol. Chem.* **280**, 9769–9772 (2005).

35. E. Santini, C. Alcacer, S. Cacciatore, M. Heiman, D. Hervé, P. Greengard, J. A. Girault, E. Valjent, G. Fisone, L-DOPA activates ERK signaling and phosphorylates histone H3 in the striatonigral medium spiny neurons of hemiparkinsonian mice. *J. Neurochem.* **108**, 621–633 (2009).

36. G. C. Scheper, C. G. Proud, Does phosphorylation of the cap-binding protein eIF4E play a role in translation initiation? *Eur. J. Biochem.* **269**, 5350–5359 (2002).

37. M. Buxade, J. L. Parra-Palau, C. G. Proud, The Mnks: MAP kinase-interacting kinases (MAP kinase signal-integrating kinases). *Front. Biosci.* **13**, 5359–5373 (2008).

38. J. E. Dancey, Inhibitors of the mammalian target of rapamycin. *Expert Opin. Investig. Drugs* **14**, 313–328 (2005).

39. P. Svenningsson, M. Lindskog, C. Ledent, M. Parmentier, P. Greengard, B. B. Fredholm, G. Fisone, Regulation of the phosphorylation of the dopamine- and cAMP-regulated phosphoprotein of 32 kDa in vivo by dopamine D1, dopamine D2, and adenosine A2A receptors. *Proc. Natl. Acad. Sci. U.S.A.* **97**, 1856–1860 (2000).

40. K. B. J. Franklin, G. Paxinos, *The Mouse Brain in Stereotaxic Coordinates* (Academic Press, San Diego, 1997).

41. T. Schallert, J. L. Tillerson, Intervention strategies for the degeneration of dopamine neurons in parkinsonism: Optimizing behavioural assessment of outcome in *Central Nervous System Diseases: Innovative Models of CNS Diseases from Molecule to Therapy*, D. F. Emerich, R. L. Dean III, P. R. Sanberg, Eds. (Humana Press, Totowa, NJ, 2000), pp. 131–151.

42. H. Towbin, T. Staehelin, J. Gordon, Electrophoretic transfer of proteins from polyacrylamide gels to nitrocellulose sheets: Procedure and some applications. *Proc. Natl. Acad. Sci. U.S.A.* **76**, 4350–4354 (1979).

43. G. L. Snyder, J. A. Girault, J. Y. Chen, A. J. Czernik, J. W. Kebabian, J. A. Nathanson, P. Greengard, Phosphorylation of DARPP-32 and protein phosphatase inhibitor-1 in rat choroid plexus: Regulation by factors other than dopamine. *J. Neurosci.* **12**, 3071–3083 (1992).

The following resources related to this article are available online at http://stke.sciencemag.org.
This information is current as of April 20, 2017.